Journal of Engineering and Science Research 6 (6): 88-98, 2022
e-ISSN: 2289-7127

DOI: 10.26666/rmp.jesr.2022.6.9

Numerical Simulation of Wear in Aircraft Carbon-Carbon Composite Disk Brake

E M.Ramadan [1,*], Ahmed E.Hussien [2], Amro M.Youssef [3] and Tarek M.Abd El-Badia [4]

[1,2,3,4] Military Technical College, Mechanical Design and Production Department, Cairo, Egypt
*Corresponding Author: eramadan@mtc.edu.eg; eramadan199194@gmail.com Tel.: +201007086975

Received: 01 November 2022; Revised: 05 November 2022; Accepted: 30 November 2022; Published: 30 December 2022

Abstract: Friction and wear are two major factors affecting the disk brake service life. Carbon-carbon composite materials have good stable friction properties, which enable them to operate as friction material in aircraft brakes application. This article discusses a wear simulation method for predicting the wear amount of c/c composite aircraft brakes under simulated operating conditions. A modified version of Archard's wear equation is used in 2-D axisymmetric finite element model in order to predict the disk brake friction surfaces wear progression. The finite element commercial software COMSOL Multiphysics 5.5 is used to simulate wear and is presented in this paper. Wear law was implemented as a boundary ordinary differential equation (ODE) in a COMSOL Multiphysics simulation, considering wear depth (thickness) as the independent variable. Frictional heat generation is simulated as heat affects on material thermal properties and as a result surface deformation. Element removal technique is used to simulate the brake disk geometry thickness change due to the material loss during wear. Wear progression with time is presented. Wear model is verified using experimental work from literature.

Keywords: *Wear, Friction, Finite Element, Carbon- Carbon Composite*

1. Introduction

Product service life is usually affected by the material loss factor. Wear is described as loss of material from the surface due to the relative motion between the working components [1]. During wear of material frictional heat generation is produced, deformation in the contacting regions and presence of contaminants and wear debris therefore, it is very complex to model the wear criteria[2, 3]. Enormous research has been performed to produce a wear model which can describe different wear modes[4].

Archard's wear model was the first model to describe the sliding wear as this model was created depending on dimension analysis [5, 6]. Archard's model is based up on relative motion between two contacting surfaces in opposite motion, as there are asperities in the two surfaces. Archard focused on the contact mechanics and depended on number of parameters for his model which are the applied stress in the contact region and the relative sliding distance between the contacting surfaces. Archard assumed that plastic deformation will occur and material properties (hardness) will affect wear rate of both soft and hard material[7]. Archard's predictive equation has been used and cited in many scientific research papers [1, 8-10]. Extensive theoretical and analytical research have followed Archard's work. There is no single predictive wear equation which can be used for practical use [11, 12]. By developing of different finite element software, this was an important opportunity to simulate the wear rate of sliding surfaces. Many studies have used finite element simulation to study the sliding wear. Molinari et al have used a finite element model studying the dry sliding wear using modified archard's wear equation[13]. Progress of wear model was also simulated in many articles for many materials [14-16].

Tribological behavior for c/c composite was studied showing effect of varying parameters such as applied load,

Corresponding Author: E M.Ramadan, Military Technical College, Mechanical Design and Production Department, Cairo, Egypt.
Email: eramadan@mtc.edu.eg

sliding speed and sliding distance [8, 17, 18] also effect of fiber orientation, fiber type, fiber size and length, heat treatment process and construction of the c/c composite was studied as it is an important factor affecting the tribological behavior [19-21]. Carbon-carbon composite material has low density, great thermal properties, good mechanical properties and self-lubricating abilities. c/c composite material is used in jet fighters such as f-14,f-15,f-16,f-18 and French mirage 2000 as well as commercial aircrafts such as Boeing 747 , and gulf stream[17, 18, 22-24]. Aircraft brake simulation work is limited owing to the difficulty of obtaining aircraft specifications and landing situations. In this article, c/c composite brake disks will be simulated during its operation in aircraft where the wear rate during landing operation can be detected for all brake disks in the whole stack.

Using COMSOL Multiphysics software the finite element wear model will be built to present the contact pressure between the stator and rotor disks, the wear rate and as a result the service life for the brake disks. This model depends on detecting the thickness of brake disks due to wear and remeshing to update the disk thickness and surface geometry. This technique will provide a real contact pressure between the disks after material removal.

2. Wear Model Simulation

In order to simulate the progressive wear depth in brake disks the finite element analysis is used to calculate the contact pressure fields and then a modified version of Archard's wear equation is used to simulate the wear phenomena.

2.1. Wear Modified Equation

Archard's wear law regarded that the sliding velocity and contact pressure affect on the wear rate of the materials in contact [1, 5, 17, 19]. The height variation of the disks will be an indication for material wear. The reduction in thickness of the brake disks due to material loss is direct proportional to the local contact pressure, local sliding velocity and wear coefficient. This wear equation is implemented in the finite element analysis with respect to time as.

$$\frac{\Delta h}{\Delta t} = k\, p(t)\, v(t) \qquad (1)$$

P is the contact pressure between friction surfaces, v(t) is the sliding velocity and k is wear coefficient. Wear coefficient is assumed to be constant for all the braking operation and for the finite elements as currently there is no suitable method for predicting the wear coefficient for every local element during the braking action.

2.2. Wear Modeling Procedure

In the form of a closed loop, the finite element wear simulation process is carried out as shown in Fig. 1. It starts with simulating the contact mechanics physics for the finite element which includes modelling the brake disks geometry of the contact, providing material properties and applying boundary conditions. The status of each node on the contact surface (closed or open) is obtained by reading the FE results from the contact simulation and the contact pressure at each surface node is calculated. The modified archard wear equation is used to simulate wear process as an ordinary differential equation inside the model where the sliding velocity of every local element is known and consequently the reduction in thickness of the disks can be calculated.

The local wear depths are not the same at each surface node, implying that the shape of the contact surface changes over time. However, with the applied pressure and the incremental wear, the contact surface is considered to be smooth for the upcoming iteration. The wear depth for the frictional contact surfaces is calculated as the averaged value for the local wear depths at every surface node.

A certain technique is used to simulate the material loss during the wear simulation process. As when a certain layer of the material is removed (thickness reduction) resulted from wear modeling the model start to update the geometry with the new height and this will guarantee a real distribution for the contact pressure. Elements of the surface layer of each contact surface are extracted from the finite element model according to the amount of material loss at this wear-iteration and no further element calculations are performed for the extracted elements, which decreases the overall calculation time.

The new geometry is remeshed to compute the contact pressure and to simulate the wear process again where all this operation is done in a closed loop till the end of braking operation [2, 21, 25].

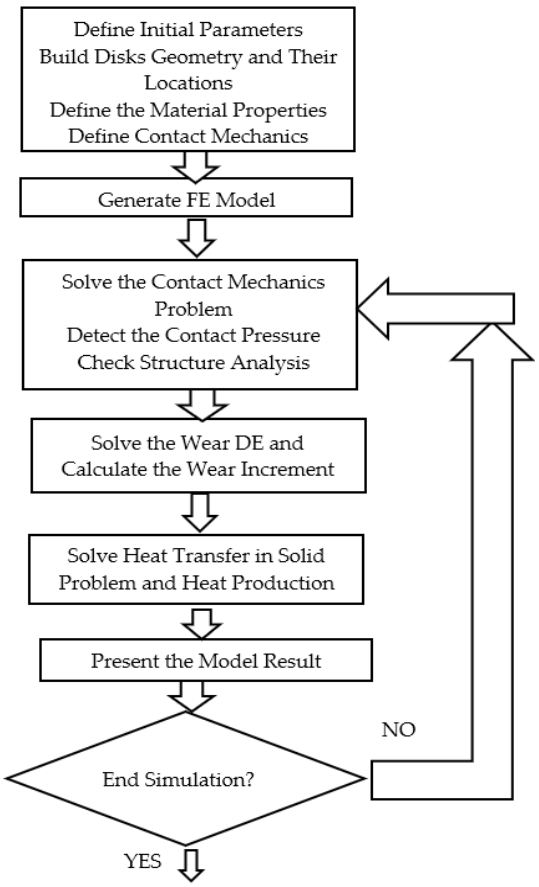

Figure 1. Aircraft brake model flow chart

3. Aircraft Brake Model

Aircraft brakes consist of a number of disks rotors that are driven by wheels and placed between stators that are kept stationary by the braking structure as shown in Fig. 2. By using hydraulic power and compressing the disks, the braking action was achieved. As pressure is applied, fluid enters the housing inlet ports, which will force the pistons against the pressure plate assembly. This movement of pressure plate will compress the disk brakes against torque tube causing friction between stator disks and rotor disks. This friction will retard and reduce the speed of wheels and stop the aircraft. During this braking operation wear will occur, therefor c/c composite will be simulated under effect of the aircraft braking conditions. During braking operation heat is generated, which should be dissipated as it will affect the contact pressure between the disks and therefor the wear depth.

Rotors connected to wheel

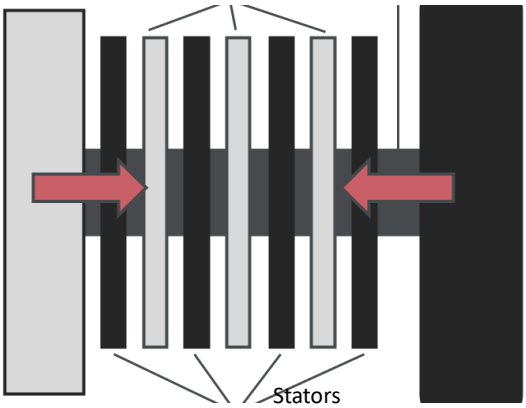

Figure 2. Aircraft brake assembly

3.1. Disk Brake Geometry and Material

Aircraft brake consists of seven disks as shown in Fig. 3 three rotating disks surrounded by four stationary disks. The hydraulic actuating system applies an axial force to a set of disks. This model is simulated in 2D axisymmetric problem without sacrificing results accuracy. It is used in this way to reduce the computation time and storage. The hydraulic pressure is uniformly distributed across the pressure plate's surface. Fixed constrain has been taken into consideration to prevent the movement of the back plate in the vertical direction due to axial force applied on the pressure plate. The pistons housing and torque tube has been neglected in the simulation model.

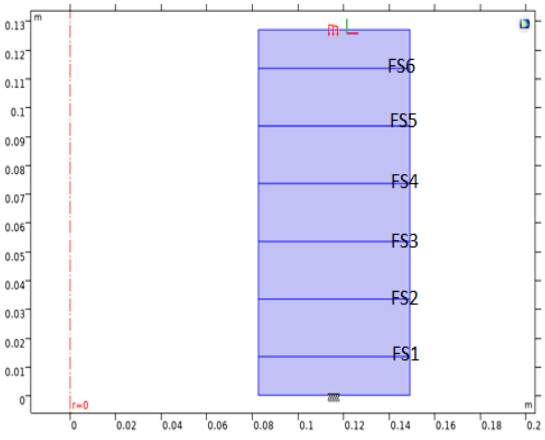

Figure 3. 2D Axisymmetric aircraft brake model friction surfaces

Both the stator and the rotor disks have the same dimension also the back plate and the end plate have the same dimension, as these two disks need only one-friction surface are shown in Table 1. Carbon-carbon composite isotropic material properties [25] are shown in Table 2.

Table 1. Disk brake dimensions

Disk type	Inner diameter (mm)	Outer diameter (mm)	Thickness (mm)

Stator and rotor disks	82.5	149	20
Back plate and end plate	82.5	149	13

Table 2. C/C composite material properties

Material property	disk
Density, (kg/m^3)	1800
Modulus of elasticity, Er (GPa)	50.9
Modulus of elasticity, Ez (GPa)	5.89
Poisons ratio, υrϴ	0.3
Poisons ratio, υrz	0.33
Shear modulus, Grz (GPa)	2.46
Thermal conductivity, kr (W/mK)	50
Thermal conductivity, kz (W/mK)	10
Heat capacity, cp (J/kg.K)	1420
Thermal expansion, αr (10^{-6}/K)	0.31
Thermal expansion, αz (10^{-6}/K)	0.29
Density, (kg/m^3)	1800
Modulus of elasticity, Er (GPa)	50.9
Modulus of elasticity, Ez (GPa)	5.89

All the disks are made from the same material with the same manufacturing process. Aircraft brakes are used to decelerate the aircraft speed during landing or rejected take off conditions and this will generate heat on friction surfaces. Aircraft deceleration is assumed to be constant and as a result the speed decreases linearly with time during the braking process.

3.2. Finite Element Model

COMSOL Multiphysics finite element commercial software is used to build a 2-D axisymmetric model to simulate the wear for c/c composite aircraft brake disks. Friction contact surfaces are the heat sources in the disk brakes during braking and also material losses takes place from these friction surfaces. Contact between the disks should be defined clearly as a source and destination for the contacting surfaces. Using solid mechanics physics all loads and constrains can be defined on the boundary or domain, as it is used to define the pressure applied from the hydraulic system to the pressure plate. Fixed constrain is defined to the boundary of the back plate. six contact pairs were defined for six friction surfaces labeled as in Fig. 4 FS1, FS2, FS3, FS4, FS5 and FS6. The contact pressure method used for detecting pressure transferred between plates is augmented lagrangian method.

A modified version of archard's wear equation is used to detect material losses. For defining such a differential equation in COMSOL Multiphysics ODE (ordinary differential equation) was used where it is defined on every friction surface. The result give indication about the depth of wear for every finite element. In order to increase the accuracy of the results for wear model finer mesh is used with increasing the number of elements at the contact surfaces to get better accurate results during mesh building as shown in the Fig. 4.

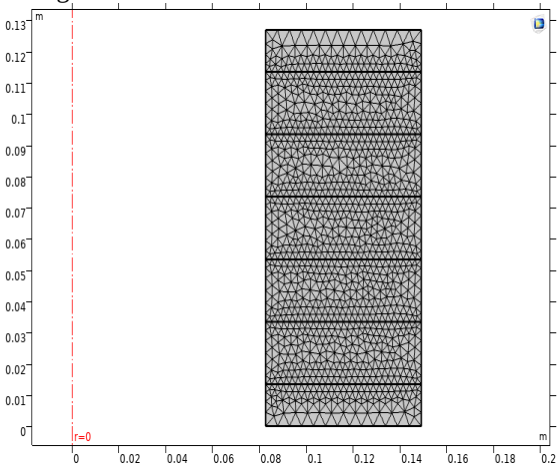

Figure 4. 2D Axisymmetric model showing the mesh build

3.3. Braking Torque and Heat Dissipation Calculation

In any mechanical system, the heat dissipated to stop or slow down the vehicle is equivalent to the energy extracted from the system. The mechanical equivalent of heat is equal to the change in kinetic energy during braking interval and also the work added to the system if presented.

In case of stopping aircraft, the total energy can be calculated as:

$$E = \frac{1}{2} N I \omega^2 + \frac{1}{2} m v^2 + Wa \quad (2)$$

$$W = \Delta E = \Delta KE + Wa \quad (3)$$

Where E is the total energy, W is the total work for achieving the change in energy (for stopping the vehicle), ω is angular velocity, I is wheel mass moment of inertia, N number of wheels, m is the total aircraft mass , Wa represent the work added to the system whatever it is positive or negative work [26] .

The kinetic energy generated by wheel rotation is frequently insignificant in comparison to the translational kinetic energy [26] therefore, the brake retardation power is calculated by the first derivative of the vehicle kinetic energy:

$$P = -m\, v(t)\, a(t) \quad (4)$$

where m is the total aircraft mass, v(t) is the aircraft speed and a(t) is the deceleration.

The heat power per unit area is calculated from the following equation:

$$q = \mu P v(t) \quad (5)$$

where q is heat power of friction surfaces per unit area, P is specific pressure between brake discs, $v(t)$ is the aircraft speed and μ is the friction coefficient during braking.
Heat flow between disks are governed by heat equation which describes the heat flow between disks as shown:

$$\rho\, c\, \frac{\partial T}{\partial t} + \nabla(-k\nabla T) = \rho\, c\, v.\Delta T \quad (6)$$

Where ρ the density of the disks material, c is the heat capacity of the disks material, k is the thermal conductivity of the disks material, v is the local velocity vector of the disks [2, 3, 27].
During aircraft braking air is forced towards the brake disks with velocity assumed to be the same as the aircraft velocity, this act as forced convection which work on dissipating the heat energy due to braking. To account for heat dissipated to the ambient environment, heat transfer by forced convection is defined on all boundaries and is calculated as:

$$q = h\,(T_{ex} - T) \quad (7)$$

Where q is heat flux across the surface due to forced convection, h is heat transfer coefficient, T_{ex} is external surface temperature and T is the ambient temperature [2, 3, 27].
Heat is dissipated to the surrounding by radiation and is taken into consideration for all the disks boundaries as

$$q = \varepsilon\, \sigma\, (T_{sur}^4 - T^4) \quad (8)$$

Where ε is the emissivity, σ is the Stephan Boltzmann constant and T_{sur} , T are temperature of the disks and surrounding[2, 3, 27].
Work done to stop the aircraft is converted into heat between the friction surfaces. The braking torque required to slow down the aircraft at constant deceleration is related to the total work done for stopping the aircraft

$$W = \frac{(\omega o + \omega f)}{2}\, T\, t \quad (9)$$

Where T braking torque, ωo is initial angular velocity, ωf is the final angular velocity and t is the braking time.
The braking pressure is the main cause of the braking torque as the pressure plate compresses the disks with certain pressure resulting in braking torque and this torque can be calculated as:

$$T = \frac{2\, n}{3\sqrt{3}}\, \mu\, P\, r_o^3 \quad (10)$$

Where n is number of contact faces, μ is material friction coefficient, P is the contact pressure and r_0 is the outer radius for brake disk [26].

4. Wear Model Validation

Wear model validation was applied depending on the experimental work done by lee et al[23]. They used a homemade friction and wear testing machine in air to test the material by applying a disk on disk sliding wear test. Both the rotor and stator test specimens are made from the same material with same dimensions inner radius 5 mm outer radius 12.5 mm and thickness 5 mm.

The motor was used to accelerate the speed of the rotor test specimens until reaching the desired value (1400, 2000 RPM) then power of the motor is shut off, and then brakes are applied under certain pressure (1.7MPa) to stop it. The results showed that the time required to stop a rotor specimen with speed 1400RPM and 2000 RPM were 26 sec and 40 sec respectively.

The wear coefficient was calculated depending on Archard's wear equation as the weight loss can be detected by measuring the specimens weight before and after the test[8, 28].

$$k = \frac{V}{F\, v\, t} \quad (11)$$

Where V is the wear volume, F applied load, v is the sliding velocity and t is time.

lee et al [23] showed that for stopping the rotor test specimen with speed of 1400RPM the weight loss was 1mg with wear coefficient 4.73×10^{-14} Pa^{-1} . Also, during stopping rotor specimen with speed of 2000 RPM the weight loss was 2mg with wear coefficient 4.3×10^{-14} pa^{-1}. Zaho [2] also validated his model to the experimental work done by lee et al [23] as zaho build his simulation model using abacus software. Zaho results for stopping the rotor specimen with speed of 1400 RPM the wear depth was 1.320 μm in 26 sec and for stopping the rotor specimen with speed 2000 RPM the wear depth was 2.643 μm in 40 sec that give the weight losses of 0.985 mg and 1.972 mg respectively. This work was simulated in our model developed using COMSOL Multiphysics in order to validate the simulation model. Results for FE model showed that simulating the speed of 1400, wear depth was 1.41 μm which equal to weight of 1.05 mg as shown in Fig. 5.

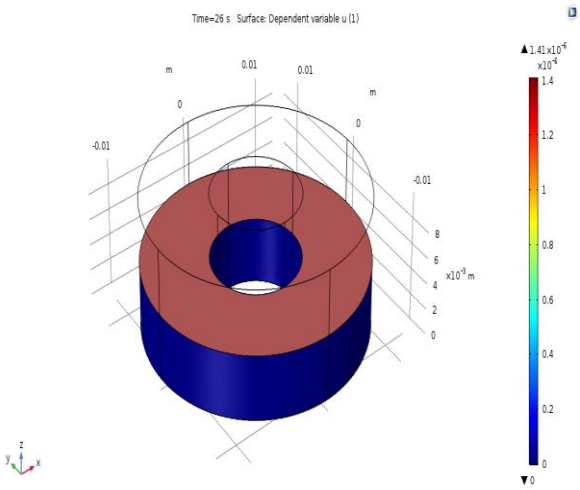

Figure 5. Wear model validation using the speed of 1400 RPM

In addition, the results for simulating speed of 2000 RPM showed that the wear depth was 2.73 μm at time 40 sec that equal to weight losses of 2 mg as shown in Fig. 6. From the results shown in Fig. 4 and Fig. 5 it can be deduced that this finite element model can predict the amount of wear for aircraft brakes.

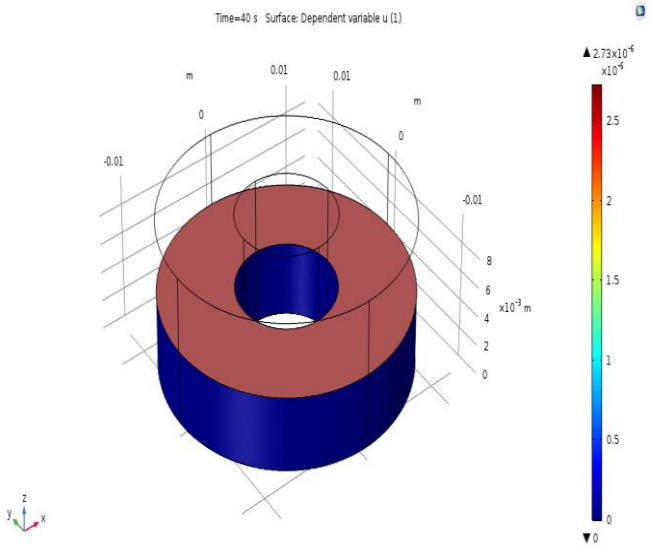

Figure 6. Wear model validation using the speed of 2000 RPM

5. Selected Case Study

A fighting aircraft with the following landing conditions in table 5.4 will be simulated. Table 5.4 is presenting the aircraft mass, landing speed, deceleration rate, environmental temperature, braking time, braking pressure calculated from the braking torque and energy change to stop the aircraft.

Wear coefficient is detected in laboratory for the c/c composite brake material using universal friction and wear testing machine under the simulated braking conditions.

Table 3. Aircraft braking conditions

Material property	disk	
m_plan	9000[kg]	Aircraft Mass
r_wheel	0.352[m]	Wheel Radius
v0	260[km/h]	Initial Aircraft Touch Down Speed
a0	-3.611[m/s^2]	Initial Vehicle Acceleration
T_air	300[K]	Air Temperature
t_brake_start	1[s]	Braking Time (Start)
t_brake_end	21[s]	Braking Time (End)
k	7×10-14[Pa^{-1}]	WEAR COEFFICIENT
P	0.7[MPa]	Braking Pressure

Aircraft velocity is defined as linear equation decreasing with time due to braking pressure as in Fig. 7. Aircraft deceleration for reducing the speed of aircraft until stopping is defined in an analytic function as a constant value during the whole braking operation as shown in Fig. 8.

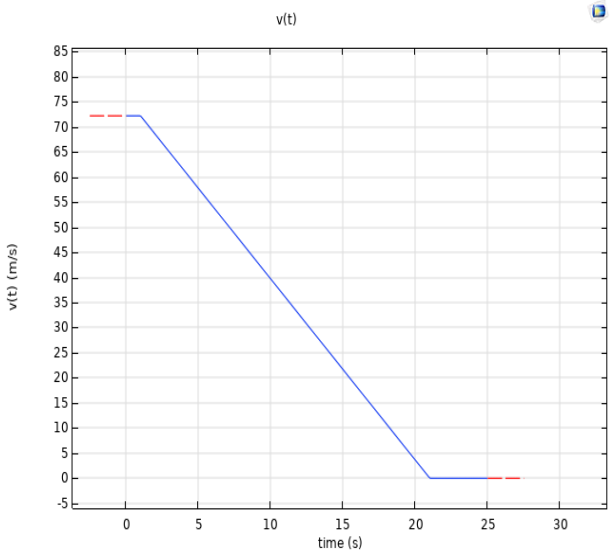

Figure 7. Aircraft velocity during braking

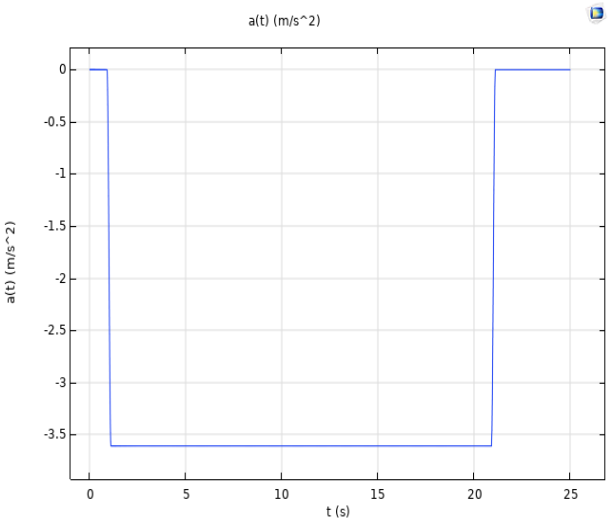

Figure 8. Aircraft deceleration during braking

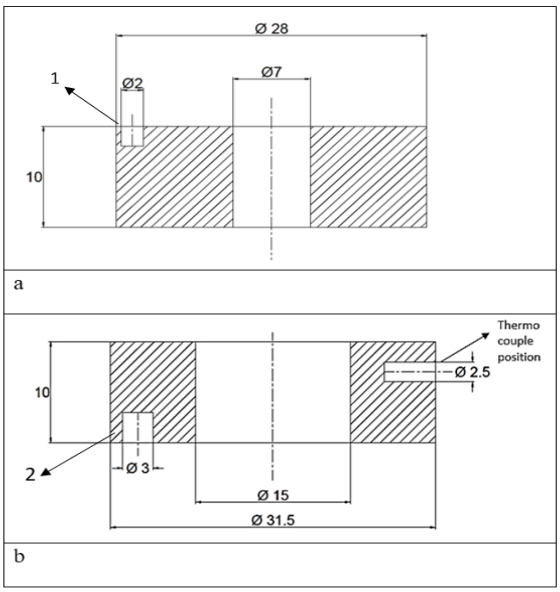

Figure 10. (a) stationary test specimen, (b) Rotating test specimen

6. Wear Coefficient Detection

A universal friction and wear testing machine in Fig. 9 is used for testing c/c composite by achieving dry disk on disk sliding wear test.

Figure 9. Universal friction and wear testing machine MMW-a1

Rotor and stator test specimens dimensions are shown in Fig. 10a and Fig. 10b in mm respectively with the fixation holes for the specimen holder. Point (1) and point (2) in Fig. 10 (a) and (b) show fixations for both rotor and stator test specimens.

Experiments are performed under air with relative humidity ranging between 45% and 55% and under the following testing parameters applied load of 0.7 MPa, rotating speed 1910 rpm and testing time of 12 min.

A thermo couple was used to measure the temperature due to friction as shown in Fig. 10(b). It was inserted under the friction contact surface by 2mm in the stator test specimen. During achieving the experiment, friction torque is measured and coefficient of friction is obtained. The weight loss was measured using a four-digit weighting balance as the experiment was done three times, the weight for every experiment was measured three times, and average value was recorded.

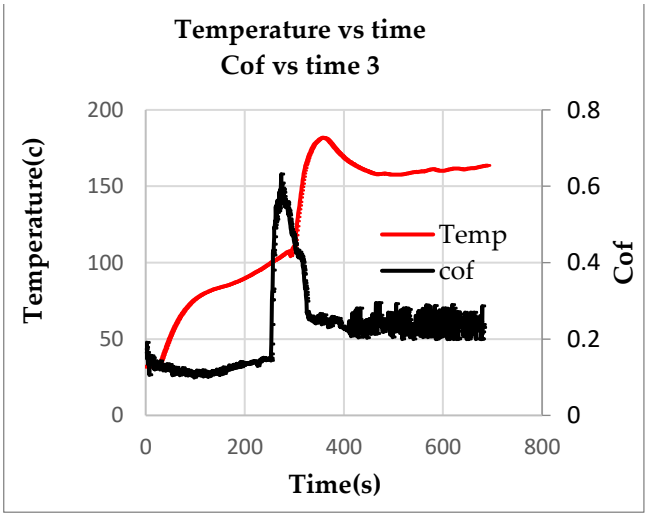

Figure 11. Temperature, coefficient of friction vs time.

During testing, as shown in Fig. (11) C/C composite materials had transition occurrence at temperature of 150°c where the friction coefficient increases sharply from 0.1 up to 0.6 and then decreases again to 0.25. This transition occurred when the removed abrasive particles start to affect both friction surfaces. By increasing heat and under the applied pressure, these abrasive particles will form a fine lubricant layer of powder reducing the friction coefficient which will act as lubricant between both surfaces. This phenomenon give the C/C composite material the advantage of self-lubricating to reduce the material loss due to friction and these results were matched with blanco [19].

The average coefficient of friction measured value is 0.2427 and wear coefficient is detected depending on Archard's wear equation and is found to be $7E^{-14}$. During studying this issue, the friction coefficient value was found to be assumed as a constant value in many related researches [2, 3, 25, 29]. Although there is a graph representing the relation between friction coefficient changes during the testing and temperature increase due to friction, friction coefficient was assumed to be constant as it was difficult to get a certain accurate equation representing the relation between the friction coefficient and the temperature for the specified material.

7. Results

The model is built to simulate the actual braking operation, which starts by applying brake pressure, which will cause material losses and heat production due to friction. The contact pressure between the friction surfaces is not constant during the whole braking operation although the hydraulic pressure affecting on the disks is constant.

The contact pressure between friction surfaces shows non-uniform pressure distribution on the contact areas as pressure progresses from the middle of friction surfaces to the ends of the disks as shown in Fig. 12.

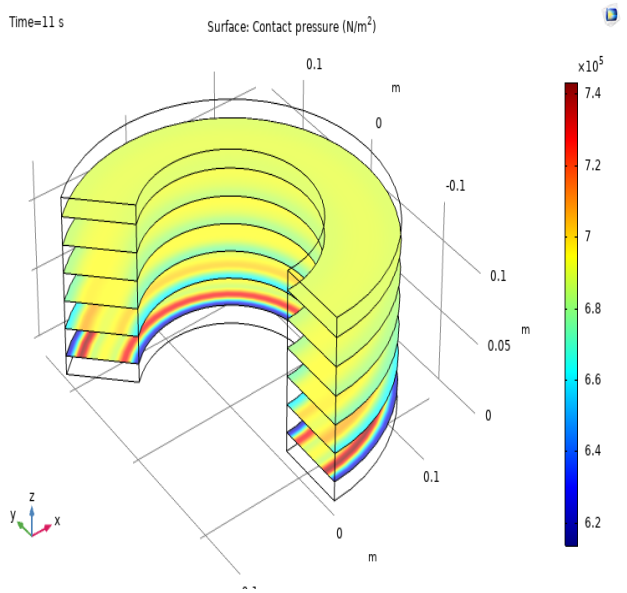

Figure 12. Contact pressure between contacting surfaces at t=11sec

Fig. 13 shows the contact pressure over the disk radius for FS6 during the braking operation where the pressure distribution changes with time for the single friction surface. The pressure value progresses from the center to the end of the disk, these changes affects on material loss and surface morphology. As shown in Fig. 13 the contact pressure is very high at the center of the contact area and low at the ends, which means loss of contact. In comparing pressure distribution for different friction surfaces as in Fig. 13 and Fig. 14 it can deduced that pressure distribution is changing during braking for all friction surfaces. Sudden decreases in contact pressure are observed at the inner and outer radii, which indicate a loss of contact or diminished contact. These changes are due to temperature effect on the disk brake material where the disks temperature increase due to heat generation and friction between the disks. This increase in temperature also affects the material properties.

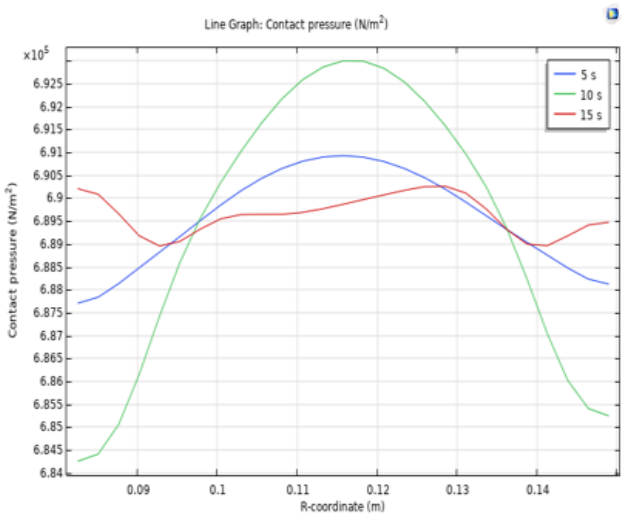

Figure 13. FS6 Contact pressure vs disk radius at different selected times

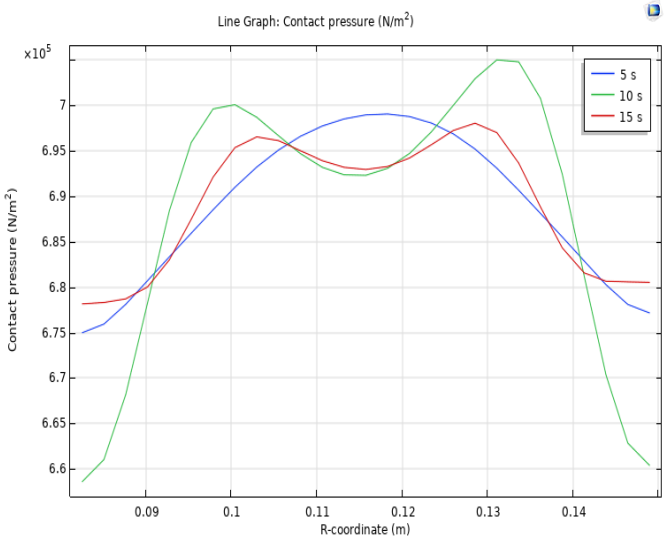

Figure 14. FS2 Contact pressure vs disk radius at different selected times

The outer disk (FS1, FS2, FS5 and FS6) showed less temperature rise due to better heat dissipation to the surrounding. While, the middle rotor disk (FS3 and FS4) exhibit higher temperature rise, which affects the thermal deformation, contact pressure and the wear rate on those disks. The brake disks temperature at t=21 sec is high at the middle rotor disk at fs3 and fs4, while it has a lower value at the pressure plate and end plate as shown in Fig. 15.

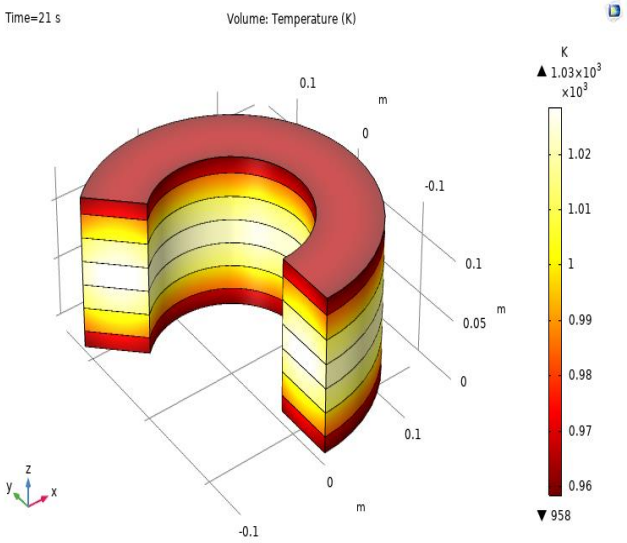

Figure 15. Disk brake temperature at end of braking operation

Also, non-uniform contact pressure distribution between disks causes non-uniform temperature at the surfaces as shown in Fig. 16 that will effect on deformation and consequently the wear of the disks. The lower temperatures of the inner and outer radii (disk ends) of the annular disks in comparing to the interior friction surfaces at the middle of the disk as this is referred to heat dissipation. The outer surfaces of the disks show lower temperature due to better heat dissipation to the surrounding by thermal convection and radiation.

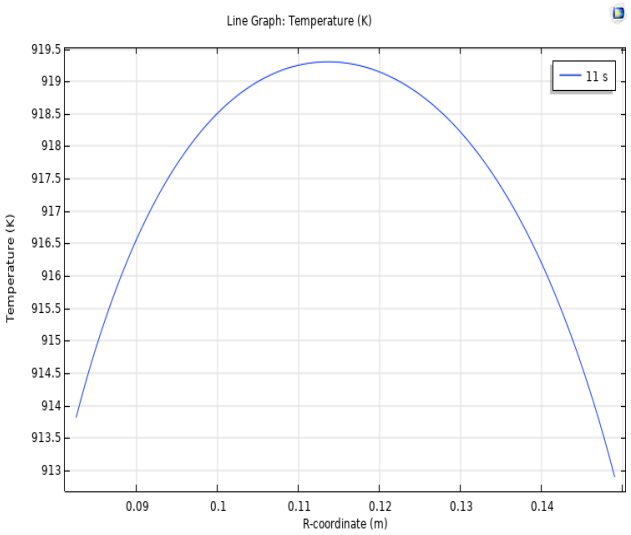

Figure 16. Temperature vs disk radius for fs3 at t=11sec

Wear depth is presented in Fig. 17 for the contacting surfaces at t=21sec during the braking operation for the aircraft. The non-uniformity of wear depth of the frictional surfaces is referred to the non-uniform contact pressure and change of sliding velocity along the disk radius. It is clearly viewed that the wear depth increases moving from the inner

radius to the outer radius as the sliding speed increases near to the outer radius. At the end of the braking operation, the highest wear value that the disks will reach is 14.7 µm. According to archard's wear equation the contact pressure and the sliding speed affect the friction surface wear amount.

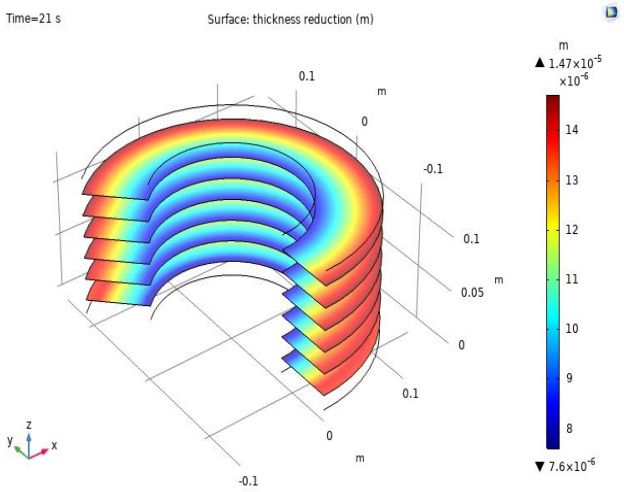

Figure 17. Wear depth for disk brakes contacting surfaces at t=21sec

Fig. 18 shows the wear depth for certain elements on FS1 along the disk brake radius. The wear depth is not the same along a given friction surface. An average value for these nodal wear values is calculated and used in the element removal technique for future calculation.

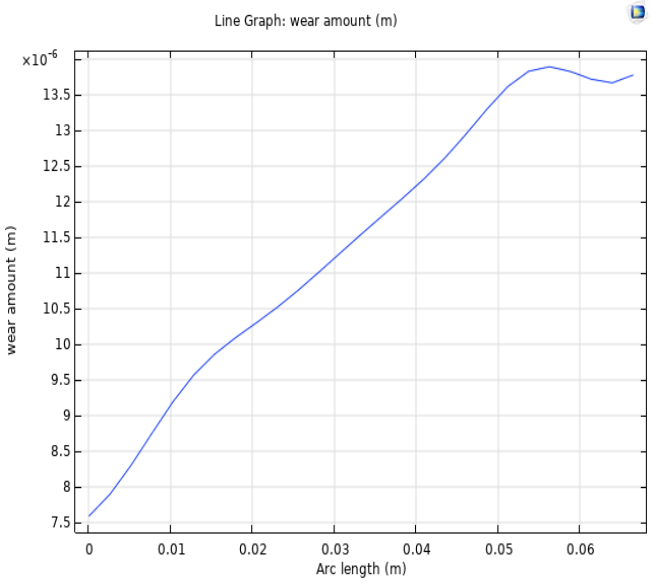

Figure 18. FS1 wear amount vs disk brake radius at t=20sec

Wear depth of material during the whole braking operation for FS1 for every certain second is presented in Fig. 19. The wear rate decrease with braking time is explained by the reduction of aircraft speed.

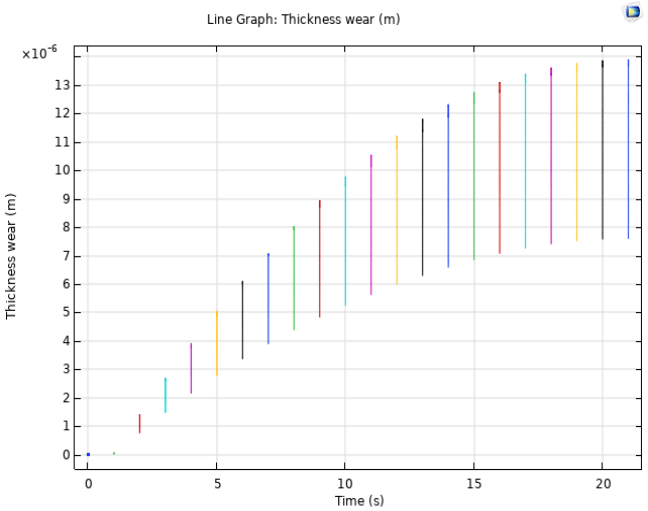

Figure 19. Fs1 wear depth variation vs time during braking operation

Fig. 19 shows wear depth increment with time for FS1, wear depth for every certain second for FS1 is showed in steps where the lower value represents the inner radius and the highest value represent the outer radius. while the wear depth is increasing near to the outer radius because of the sliding speed is increasing also. The wear depth slope is decreasing because the sliding velocity is decreasing with time. Frictional heat generation and wear amount will also decrease as the sliding speed is decreasing.

8. Conclusion

Numerical simulation and investigation for the wear of c/c composite multidisc brake in aircraft during braking operation has been performed using finite element method. The model was based up on contact pressure between the disks and the modified version of archard's wear equation.

Frictional heat generation and heat dissipation by forced convection and radiation were defined in the model where this will affect on the contact pressure between friction surfaces and the wear amount. The material removal technique is used to update the surface geometry and remeshing. Archard's wear law have been applied at each node at the contact surfaces.

From the contact pressure between the disks it has been observed that pressure value varied from the applied pressure increasing and decreasing. Thermal properties affect the wear amount as the frictional heat generation will increase the disks temperature. Heat dissipation affect the wear amount as it will affect the contact pressure distribution. Contact pressure variation due to heat generation is because of material thermal deformation. Material wear rate graphs

explained that material wear increases near to the disk outer radius as the sliding speed increase.

Acknowledgements

The corresponding author is very grateful to the experts of the other authors for their appropriate and constructive suggestions to improve this scientific paper.

REFERENCES

[1] B. Bhushan, *Principles and applications of tribology*. John Wiley & Sons, 2013.

[2] S. Zhao, G. E. Hilmas, and L. R. Dharani, "Numerical simulation of wear in a C/C composite multidisk clutch," *Carbon,* vol. 47, no. 9, pp. 2219-2225, 2009.

[3] S. Zhao, G. E. Hilmas, and L. R. Dharani, "Behavior of a composite multidisk clutch subjected to mechanical and frictionally excited thermal load," *Wear,* vol. 264, no. 11-12, pp. 1059-1068, 2008.

[4] H. Meng and K. Ludema, "Wear models and predictive equations: their form and content," *Wear,* vol. 181, pp. 443-457, 1995.

[5] J. Archard, "Contact and rubbing of flat surfaces," *Journal of applied physics,* vol. 24, no. 8, pp. 981-988, 1953.

[6] J. Archard and W. Hirst, "The wear of metals under unlubricated conditions," in *Proceedings of the Royal Society of London A: Mathematical, Physical and Engineering Sciences*, 1956, vol. 236, no. 1206: The Royal Society, pp. 397-410.

[7] S. Montgomery, D. Kennedy, and N. O'Dowd, "Analysis of wear models for advanced coated materials," 2009.

[8] J. Gomes, O. Silva, C. Silva, L. Pardini, and R. Silva, "The effect of sliding speed and temperature on the tribological behaviour of carbon–carbon composites," *Wear,* vol. 249, no. 3, pp. 240-245, 2001.

[9] A. Söderberg and S. Andersson, "Simulation of wear and contact pressure distribution at the pad-to-rotor interface in a disc brake using general purpose finite element analysis software," *Wear,* vol. 267, no. 12, pp. 2243-2251, 2009.

[10] K. Friedrich, R. Reinicke, and Z. Zhang, "Wear of polymer composites," *Proceedings of the Institution of Mechanical Engineers, Part J: Journal of Engineering Tribology,* vol. 216, no. 6, pp. 415-426, 2002.

[11] S. Hsu, M. Shen, and A. Ruff, "Wear prediction for metals," *Tribology International,* vol. 30, no. 5, pp. 377-383, 1997.

[12] J. a. A. Williams, "Wear modelling: analytical, computational and mapping: a continuum mechanics approach," *Wear,* vol. 225, pp. 1-17, 1999.

[13] J. Molinari, M. Ortiz, R. Radovitzky, and E. Repetto, "Finite-element modeling of dry sliding wear in metals," *Engineering Computations,* vol. 18, no. 3/4, pp. 592-610, 2001.

[14] C. Gonzalez *et al.*, "Numerical analysis of pin on disc tests on Al–Li/SiC composites," *Wear,* vol. 259, no. 1-6, pp. 609-612, 2005.

[15] N. H. Kim *et al.*, "Finite element analysis and experiments of metal/metal wear in oscillatory contacts," *Wear,* vol. 258, no. 11-12, pp. 1787-1793, 2005.

[16] V. Hegadekatte, N. Huber, and O. Kraft, "Finite element based simulation of dry sliding wear," *Modelling and Simulation in Materials Science and Engineering,* vol. 13, no. 1, p. 57, 2004.

[17] J. Chen and C. Ju, "Effect of sliding speed on the tribological behavior of a PAN-pitch carbon-carbon composite," *Materials chemistry and physics,* vol. 39, no. 3, pp. 174-179, 1995.

[18] J. Chen, J. C. Lin, and C. Ju, "Effect of load on tribological behaviour of carbon-carbon composites," *Journal of materials science,* vol. 31, no. 5, pp. 1221-1229, 1996.

[19] C. Blanco, J. Bermejo, H. Marsh, and R. Menendez, "Chemical and physical properties of carbon as related to brake performance," *Wear,* vol. 213, no. 1-2, pp. 1-12, 1997.

[20] J. Rao, K. Sinnur, and R. Jain, "Effect of weave texture of carbon fabric on mechanical, thermal and tribological properties of carbon/carbon aircraft brakes," *Int. J. Compos. Mater,* vol. 5, pp. 89-96, 2015.

[21] R. Luo, X. Huai, J. Qu, H. Ding, and S. Xu, "Effect of heat treatment on the tribological behavior of 2D carbon/carbon composites," *Carbon,* vol. 41, no. 14, pp. 2693-2701, 2003.

[22] J. D. Buckley and D. D. Edie, *Carbon-carbon materials and composites*. William Andrew, 1993.

[23] K. Lee, J. C. Lin, and C.-P. Ju, "Surface effect on braking behavior of PAN-pitch carbon-carbon composite," *Wear,* vol. 199, no. 2, pp. 228-236, 1996.

[24] B. Yen, "An investigation of friction and wear mechanisms of carbon-carbon composites in nitrogen and air at elevated temperatures," *Carbon,* vol. 34, no. 4, pp. 489-498, 1996.

[25] J.-H. Choi, J.-H. Han, and I. Lee, "Transient analysis of thermoelastic contact behaviors in composite multidisk brakes," *Journal of Thermal Stresses,* vol. 27, no. 12, pp. 1149-1167, 2004.

[26] W. C. Orthwein, *Clutches and brakes: design and selection*. CRC Press, 2004.

[27] C. Zhang, L. Zhang, Q. Zeng, S. Fan, and L. Cheng, "Simulated three-dimensional transient temperature field during aircraft braking for C/SiC composite brake disc," *Materials & Design,* vol. 32, no. 5, pp. 2590-2595, 2011.

[28] P. Podra and S. Andersson, "Simulating sliding wear with finite element method," *Tribology international,* vol. 32, no. 2, pp. 71-81, 1999.